

TABLE II. Values of the ratio  $\gamma/\gamma_F$ .

Composition At. wt. %	$\gamma$ (mJ mole <sup>-1</sup> deg <sup>-2</sup> )	$\gamma_F$ (mJ mole <sup>-1</sup> deg <sup>-2</sup> )	$\gamma/\gamma_F$
Pure copper	0.698	0.498	1.40
99% copper	0.699	0.499	1.40
98% copper	0.696	0.501	1.39
97% copper	0.696	0.504	1.38
Pure silver	0.645	0.639	1.01

the thermal effective mass which provides an indication of the amount of distortion of the Fermi surface from a sphere. For face-centered cubic structures

$$\gamma_F = 3.848 \times 10^{11} a^2 n^{1/3} \text{ (mJ mole}^{-1} \text{ deg}^{-2}\text{)}, \quad (3)$$

where  $a$  is the lattice parameter at 0°K and  $n$  is the

electron concentration. Values of the ratio  $\gamma/\gamma_F$  for the pure metals and alloys are given in Table II. The values of  $a$  at 0°K were estimated by assuming that the  $\alpha$ -phase alloys have the same coefficient of expansion as that of pure copper. It can be seen that the ratio of  $\gamma/\gamma_F$  for pure silver is very close to unity, the value characteristic of free electrons. The general trend of this ratio  $\gamma/\gamma_F$  shows a decrease from copper to silver suggesting that the Fermi surface is becoming more spherical.

#### ACKNOWLEDGMENTS

The authors wish to acknowledge the assistance of John A. Escajeda and Kenneth C. Frederick in the experimental work. This work was supported in part by the Atomic Energy Commission.

### Lattice Dynamics of Copper

S. K. SINHA\*

*Cavendish Laboratory, University of Cambridge, Cambridge, England*

(Received 21 September 1965)

A fairly extensive survey of the phonon dispersion relation in copper at room temperature has been made by means of neutron scattering. The cold-neutron time-of-flight technique was used, and the results are confined to the (001) and (110) symmetry planes of the reciprocal lattice. An interpolation formula for the dispersion relation has been obtained by making a least-squares fit of an interatomic-force-constant model to the results. However, because of the nonconvergent behavior of the parameters with the introduction of further neighbors, the values obtained for these cannot be ascribed any physical significance beyond showing that (a) nearest-neighbor interactions dominate, and (b) the forces extend up to at least third and probably up to sixth neighbors. The frequency distribution function  $g(\nu)$  has been calculated, and the values obtained from it for the lattice specific heat and the Debye-Waller factor are in excellent agreement with experiment, except at very low temperatures. The results have been compared with calculations based on Toya's treatment (with a few minor modifications) of the electron-phonon interaction in monovalent metals. The values of the three most uncertain parameters in the theory, representing the depth of the pseudo-potential well due to the ions and the two core-overlap interaction parameters, have been obtained by fitting to the measured elastic constants. Phonon-dispersion curves calculated from these parameters show reasonably good agreement with the experimental results, especially for the transverse modes. The validity of these parameters and of the "free-electron-like" approximation for the electron wave functions, used in Toya's theory, is critically discussed.

#### INTRODUCTION

THERE has been considerable interest in the lattice dynamics of copper over the past several years, and several attempts have been made to calculate the frequency-wave-vector dispersion relation  $\nu_j(\mathbf{q})$  [ $j$ =polarization branch], and from it the frequency distribution function  $g(\nu)$ , using various theoretical models.<sup>1-6</sup>

\* Present address: Department of Physics, Iowa State University, Ames, Iowa.

<sup>1</sup> R. B. Leighton, *Rev. Mod. Phys.* **20**, 165 (1948).

<sup>2</sup> J. De Launay, *Solid State Physics*, edited by F. Seitz and D. Turnbull (Academic Press Inc., New York, 1963), Vol. 2, p. 219.

<sup>3</sup> P. L. Srivastava, *Phys. Status Solidi* **2**, 713 (1962).

<sup>4</sup> H. C. White, *Phys. Rev.* **112**, 1092 (1958).

<sup>5</sup> T. Toya, *J. Res. Inst. Catalys. Hokkaido Univ.* **6**, 161 (1958).

<sup>6</sup> G. W. Lehman, T. Wolfram, and R. E. De Wames, *Phys. Rev.* **128**, 1593 (1962).

This is partly due to the simple lattice structure of copper (face-centered cubic) and partly due to the fact that it is a monovalent metal, so that recent theories of the electron-phonon interaction<sup>5</sup> may be expected to apply to it, without the additional complications arising from several conduction electrons per atom. The frequency distribution functions obtained from many of the above models have also been used to calculate quantities like the temperature variation of the lattice specific heat and the Debye-Waller factor for copper. Comparison with the experimental values of these quantities, however, is a very insensitive test as to the validity of the models. Direct and reasonably accurate experimental observations of the dispersion relations in many crystals are now possible using the technique

of coherent inelastic scattering of neutrons.<sup>7</sup> Copper is a suitable substance for such experiments, as it has a reasonably high coherent neutron cross section, and a much smaller incoherent cross section.

This paper describes a fairly extensive survey of the phonon-dispersion relation in copper at room temperature using the neutron-scattering method. Some preliminary results have been reported elsewhere.<sup>8</sup> The dispersion relation has also previously been studied using the method of diffuse scattering of x-rays<sup>9</sup> and also using the neutron-scattering method.<sup>10</sup> Certain discrepancies with these measurements are reported. A detailed comparison of the present results with those reported by Birgeneau *et al.*<sup>11</sup> for nickel confirms their observation of the essential similarity of the dispersion relations in the two cases. This paper also presents a calculation of the frequency distribution function  $g(\nu)$  using a suitable interpolation formula for the dispersion relations, obtained by fitting an interatomic-force-constant model to the observed results. This is found to be in marked disagreement with that calculated similarly by Jacobsen<sup>9</sup> from his experimental results, but provides values for the lattice specific heat and Debye-Waller factor of copper in very good agreement with experiment.

The measured dispersion curves are examined in the light of recent theoretical treatments of the electron-phonon interaction in metals,<sup>5,12</sup> which start from more basic principles than the Born-Von Karman model. In particular, they are compared with the theoretical calculations of Toya, which have been shown to be fairly good for the case of sodium.<sup>13</sup> The agreement is not very good for the longitudinal modes. Recently Toya has recalculated the dispersion curves with modified parameters and obtained much better agreement. Toya's theory is strictly valid only for metals in which the conduction-electron wave functions are "free-electron-like," i.e., when they can be described by single orthogonalized plane waves (OPW). The band structure of copper, however, shows considerable deviation from the free-electron behavior. Further, the overlap or exchange repulsions between neighboring ion cores are large but not at all well known for copper. An attempt has been made to modify certain parameters in Toya's theory to obtain a better fit to the results, with a fair amount of success, but it is likely that the simple free-electron model used is not really valid for copper, as discussed below.

<sup>7</sup> G. Placzek and L. Van Hove, *Phys. Rev.* **93**, 1207 (1954).

<sup>8</sup> S. K. Sinha and G. L. Squires, *J. Phys. Chem. Solids*, Suppl. 1, p. 53 (1965).

<sup>9</sup> E. H. Jacobsen, *Phys. Rev.* **97**, 654 (1955).

<sup>10</sup> D. Cribier, B. Jacrot, and D. Saint-James, *Inelastic Scattering of Neutrons in Solids and Liquids* (International Atomic Energy Agency, Vienna, 1961), p. 543.

<sup>11</sup> R. J. Birgeneau, J. Cordes, G. Dolling, and A. D. B. Woods, *Phys. Rev.* **136**, A1359 (1964).

<sup>12</sup> L. J. Sham and J. M. Ziman, *Solid State Physics*, edited by F. Seitz and D. Turnbull (Academic Press Inc., New York, 1963), Vol. 15, p. 221.

<sup>13</sup> A. D. B. Woods, B. N. Brockhouse, R. H. March, A. T. Stewart, and R. Bowers, *Phys. Rev.* **128**, 1112 (1962).

## MEASUREMENTS AND RESULTS

In the inelastically scattered energy spectrum resulting from a beam of monochromatic and well-collimated neutrons incident on a single crystal, there will in general appear sharp peaks corresponding to the "coherent one-phonon processes" and these obey the basic conservation laws<sup>7</sup>

$$(\hbar^2/2m)(k_1^2 - k_0^2) = \pm \hbar \nu_j(\mathbf{q}), \quad (1)$$

$$\mathbf{Q} \equiv \mathbf{k}_1 - \mathbf{k}_0 = \mathbf{q} + \mathbf{H}, \quad (2)$$

where  $\mathbf{k}_0$  and  $\mathbf{k}_1$  are, respectively, the incident and scattered neutron wave vectors;  $\mathbf{q}$  and  $\nu_j(\mathbf{q})$  are, respectively, the phonon wave vector and the corresponding frequency of the polarization branch  $j$ ; and  $\mathbf{H}$  is a reciprocal lattice vector. The  $+$  ( $-$ ) sign refers to one-phonon annihilation (creation). Using (1) and (2), each peak in the energy spectrum of neutrons inelastically scattered in a given direction yields a point on the dispersion curve. Since copper possesses a monatomic lattice, there are only three "acoustic" branches to the dispersion relation.

The "cold neutron apparatus" on the DIDO reactor at Harwell was used for the experiments, and measurements were made using the time-of-flight technique to energy analyze the scattered neutrons. The apparatus has been described in detail elsewhere.<sup>14</sup> A collimated beam of neutrons from the liquid-hydrogen source from the reactor passes through filters of bismuth and beryllium maintained at liquid-nitrogen temperature. The emergent beam consists of neutrons with  $\lambda > 3.96 \text{ \AA}$  and contains very little fast-neutron contamination. It is then transmitted through a rotor, which serves to pulse and monochromate the beam. Under the conditions of the experiment, the mean wavelength of neutrons incident on the sample was  $4.18 \text{ \AA}$ , and the mean wavelength resolution was given by  $\Delta\lambda/\lambda = 2.8\%$ .

The neutrons scattered from the sample were detected in an array of 12 counters arranged in the same vertical plane at angles of  $30^\circ$  to  $90^\circ$  to the incident beam direction. The counters were all approximately equidistant from the sample, the mean flight path being 2.34 m. The counters used were (LiF-ZnS) scintillators, fitted with pulse-shape discriminating circuits to minimize the counting of gamma-ray background. The time-of-flight spectra in all the counters were simultaneously recorded on magnetic tape. Two monitor counters at a distance of 1.5 m apart in the incident beam recorded the time-of-flight spectrum of the incident beam, and from these the mean wavelength of the incident spectrum, and the "start time" of the neutron pulse at the rotor center were determined.

The two samples used were cylindrical single crystals of copper of length 5 cm and diameter 3.8 cm with the

<sup>14</sup> D. H. C. Harris, S. J. Cocking, P. A. Egelstaff, and F. J. Webb, *Inelastic Scattering of Neutrons in Solids and Liquids* (International Atomic Energy Agency, Vienna, 1963), Vol. 1, p. 107.

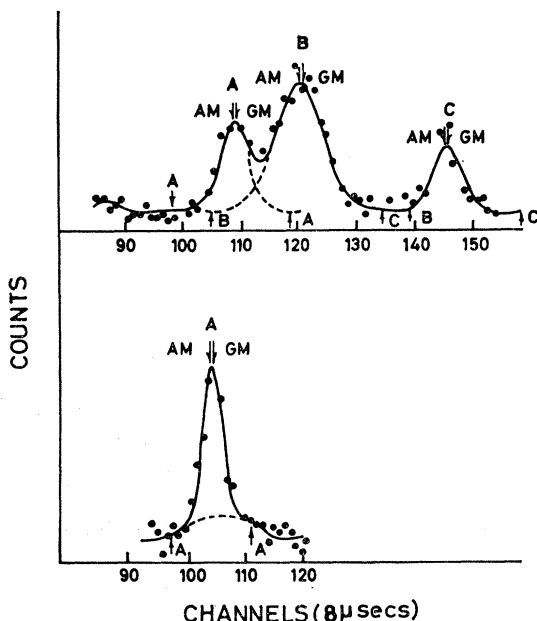


FIG. 1. Some typical time-of-flight spectra. The smooth curves represent the Gaussians fitted on a uniform background. The upper arrows represent the positions of the weighted mean times of arrival (AM) and the centers of the Gaussians (GM), respectively. The lower arrows indicate the extents within which the weighted time averages of each of the peaks were taken.

cylinder axes approximately coincident with the [001] and [110] crystallographic axes, respectively. They were purchased from Messrs. Metal Research Ltd., Cambridge, England. The experiments were done with the appropriate crystallographic axis aligned normal to the plane of scattering, whilst the crystal was rotated about this axis into different positions for successive runs, within the angular limits prescribed by crystal symmetry. Thus all the phonons measured had their wave vectors lying in either the (001) or (110) planes of the reciprocal lattice. Owing to the  $[\mathbf{Q} \cdot \mathbf{e}_j(\mathbf{q})]^2$  factor in the one-phonon coherent cross section,<sup>7</sup> [where  $\mathbf{e}_j(\mathbf{q})$  is the phonon polarization vector], points were only obtained on the two branches of the dispersion relation which were polarized in these planes.

Some typical time-of-flight spectra observed in the counters are shown in Fig. 1. These show the distinct one-phonon peaks superimposed on a background composed of a uniform part due to stray-neutron background and an energy-dependent part due to incoherent and multiphonon scattering from the sample. The one-phonon peaks are broadened due to instrumental resolution and crystal anharmonicity. In order to define a time of arrival at the counter of the neutron group scattered in the one-phonon process, the following procedure was used. A least-squares fit was made to each spectrum of a number of Gaussian peaks superimposed on a uniform background, the amplitudes, widths, and centers of the Gaussians and the magnitude of the background being left as adjustable parameters. Such a fit

is shown in Fig. 1. Broad, low-amplitude Gaussians were used to fit the incoherent and multiphonon background, whilst the sharp large-amplitude Gaussians corresponded to the one-phonon peaks. In this way, the effects of the background were approximately subtracted from the one-phonon peaks. In order to allow for the possible asymmetries in the one-phonon peaks, as were sometimes observed, the centers of the Gaussians were not used to define the mean time of arrival of the neutron group. Instead, the weighted time average of all the counts in the peak (after subtracting the background as described above) was taken, the averaging being done over an extent of 4 standard deviations on either side of the center of the Gaussian fitted to the peak. When two peaks were close enough together to be relatively unresolved, it was found to be more accurate to use the centers of the fitted Gaussians.

Because of the appreciable absorption cross section of the copper nuclei (8.12 b at 4 Å) the flight paths for both the incident and scattered beams were not taken to the geometrical center of the sample, but to the "center of scattering" in the sample. This correction was calculated separately for each measured phonon, as it depends on  $\mathbf{k}_1$ . In this way, the mean incident and scattered wavelengths corresponding to a one-phonon peak were obtained. It can be shown that with  $\mathbf{k}_0$  and  $\mathbf{k}_1$  as defined by the mean direction and wavelengths of the incident and scattered beams, respectively,  $\nu_j(\mathbf{q})$  is obtained already correct to first order in the instrumental resolution, i.e., correct to quantities of the order of  $(\Delta\lambda/\lambda)$ ,  $\Delta\theta$  etc. (where  $\Delta\theta$  is an angular resolution width). To further correct for finite instrumental resolution, second-order corrections were made to the mean scattered wavelength, to obtain the "mean one-phonon process" which corresponds to scattering of the mean incident wavelength at the mean scattering angle determined by the geometry of the apparatus. It can be shown<sup>15</sup> that the second-order correction can be expressed as a linear combination of the second moments of the different resolutions of the apparatus, in both wavelength and angular collimation. The appropriate coefficients depend in a rather complicated way on the first and second derivatives of  $\nu_j(\mathbf{q})$  with respect to  $\mathbf{q}$  and involve also the variation of the scattering cross section and counter efficiency over the peak. The corrections are appreciable only when  $|1 \pm (\hbar/2E') \nabla_{\mathbf{q}} \nu_j(\mathbf{q}) \cdot \mathbf{k}_1|$  becomes small [where  $E'$  = energy of scattered neutron, and the  $+$  ( $-$ ) sign refers to phonon creation (annihilation) processes]. In order to make these corrections, a force-constant model of the dispersion relations was used as an interpolation formula for the frequencies. This model was obtained by a preliminary fitting to the uncorrected results. The corrected results were then refitted by another force-constant model. The corrections were small and not sensitive to the model of  $\nu_j(\mathbf{q})$  so that the method was rapidly convergent.

<sup>15</sup> S. K. Sinha, Ph.D. thesis, Cambridge University, 1964 (unpublished).

The errors in frequency and wave vector were combined to give an effective error in frequency above, according to the formula,

$$\Delta\nu_{\text{eff}} = \Delta\nu - \nabla_{\mathbf{q}} \nu_j(\mathbf{q}) \cdot \Delta\mathbf{Q}, \quad (3)$$

where  $\Delta\nu$  and  $\Delta\mathbf{Q}$  are, respectively, the errors in frequency and wave vector alone. The contribution to the above expression from the different estimated errors in measuring flight paths, angles, and from the statistical error in determining the mean time of arrival of the neutron group at the counters, were squared and added separately as these errors are independent. The final result gives a single weight to any determined point on the dispersion curve. The average effective error in frequency calculated in this way for all the phonons was  $\pm 4.3\%$ , but the average scatter of the points about the fitted force-constant model was only  $\pm 2.6\%$ . The discrepancy might be due to some systematic error, but is most probably due to overestimation of some of the errors in the measured parameters.

Except for the two degeneracies along the [110] axis, the different observed branches of the dispersion relation in the (001) and (110) planes of copper are fairly well separated in frequency so that assignment of an observed point to a particular branch was not a great problem. Occasionally, it was necessary to use the  $[\mathbf{Q} \cdot \mathbf{e}_j(q)]^2$  factor in the cross section to determine the appropriate branch from the observed intensities.

Altogether 476 points were measured on the dispersion curves in both the (001) and (110) planes of the reciprocal lattice of the crystal. Table I lists all the measured phonons along the symmetry directions of the reciprocal lattice. Phonons with wave vectors lying within a  $5^\circ$  sector centered about one such direction were assigned to this direction, the frequency being interpolated by means of the fitted force-constant model to give the frequency of the phonon along the chosen direction with the same  $|\mathbf{q}|$  as the original phonon. If  $\Delta\nu_{\text{th}}$  is the change in the frequency of the fitted model from the actual  $\mathbf{q}$  to the  $\mathbf{q}$  along the chosen direction, the interpolated frequency in the symmetry direction is given by adding  $\Delta\nu_{\text{th}}$  to the actual observed frequency.  $\Delta\nu_{\text{th}}$  is usually small anyway. For brevity the off-symmetry phonons are not listed here, although they have been used in the fitting procedure outlined below.

Figure 2 shows the symmetry direction results, together with the x-ray results of Jacobsen<sup>9</sup> and the neutron-scattering results of Cribier *et al.*<sup>10</sup> Also shown are the dispersion curves calculated from the fitted force-constant model. The slopes of these fitted curves at the origin are constrained to follow those given by the room-temperature elastic constants measured by Overton and Gaffney.<sup>16</sup> It can be seen that the present results are in good agreement with these elastic constants in giving the slopes of the dispersion curves at the origin.

Large discrepancies with the x-ray results are evident,

<sup>16</sup> W. C. Overton, Jr. and J. Gaffney, Phys. Rev. **98**, 969 (1955).

TABLE I. Normal-mode frequencies of copper at 300°K. ( $q = |\mathbf{q}|$  in units of  $2\pi/a$ ; frequencies are in  $10^{12}$  cps.)

[100] T		[100] L		[111] T		[111] L		[110] T <sub>1</sub>		[110] T <sub>2</sub>		[110] L	
q	$\nu$	q	$\nu$	q	$\nu$	q	$\nu$	q	$\nu$	q	$\nu$	q	$\nu$
0.256	2.004 ± 0.16	0.226	2.710 ± 0.24	0.389	2.272 ± 0.10	0.161	2.328 ± 0.20	0.470	2.310 ± 0.07	0.213	1.778 ± 0.10	0.137	1.901 ± 0.13
0.607	4.456 ± 0.10	0.442	2.844 ± 0.27	0.495	2.649 ± 0.08	0.163	2.318 ± 0.22	0.477	2.269 ± 0.13	0.396	3.248 ± 0.22	0.254	3.462 ± 0.21
0.732	4.710 ± 0.08	0.577	3.212 ± 0.24	0.577	2.935 ± 0.08	0.209	2.907 ± 0.24	0.478	2.318 ± 0.13	0.628	4.732 ± 0.08	0.288	3.674 ± 0.26
0.701	4.789 ± 0.07	0.573	3.108 ± 0.10	0.615	3.055 ± 0.06	0.305	4.144 ± 0.28	0.581	2.831 ± 0.07	0.690	5.013 ± 0.20	0.300	4.124 ± 0.26
0.679	4.789 ± 0.07	0.439	2.908 ± 0.26	0.686	3.232 ± 0.06	0.306	4.131 ± 0.28	0.626	3.052 ± 0.08	0.756	6.713 ± 0.23	0.313	4.125 ± 0.16
0.824	4.987 ± 0.13	0.719	3.084 ± 0.23	0.693	3.237 ± 0.12	0.314	4.077 ± 0.28	0.686	3.275 ± 0.08	0.977	6.607 ± 0.48	0.386	4.692 ± 0.20
0.824	4.987 ± 0.13	0.871	3.890 ± 0.31	0.730	3.255 ± 0.08	0.319	4.127 ± 0.08	0.800	3.797 ± 0.18			0.402	4.817 ± 0.05
0.858	5.030 ± 0.11	0.961	7.211 ± 0.17	0.781	3.288 ± 0.10	0.325	6.941 ± 0.12	0.825	4.176 ± 0.74			0.428	5.126 ± 0.17
0.948	5.015 ± 0.13	0.966	7.414 ± 0.20	0.807	3.501 ± 0.06	0.686	6.941 ± 0.12	0.832	3.865 ± 0.08			0.513	5.793 ± 0.37
		0.991	7.301 ± 0.22	0.808	3.400 ± 0.10	0.736	7.177 ± 0.22	0.879	4.175 ± 0.40			0.545	5.933 ± 0.06
				0.822	3.356 ± 0.10	0.809	7.565 ± 0.22	0.907	4.238 ± 0.14			0.550	5.885 ± 0.26
								0.917	4.147 ± 0.09			0.568	6.101 ± 0.09
								0.948	4.283 ± 0.08			0.583	5.939 ± 0.27
								0.964	4.377 ± 0.13			0.592	6.007 ± 0.06
								1.041	4.565 ± 0.12			0.662	6.108 ± 0.30
								1.080	4.672 ± 0.10			0.693	6.331 ± 0.12
								1.111	4.813 ± 0.21			0.693	6.486 ± 0.19
								1.113	4.708 ± 0.10			0.862	6.346 ± 0.12
								1.140	4.900 ± 0.15			0.941	6.165 ± 0.13
								1.190	4.693 ± 0.13			1.093	5.723 ± 0.06
								1.269	5.099 ± 0.10			1.217	5.355 ± 0.07
								1.277	5.212 ± 0.15			1.318	5.177 ± 0.08
								1.302	5.095 ± 0.11				
								1.350	5.009 ± 0.28				
								1.362	5.239 ± 0.09				

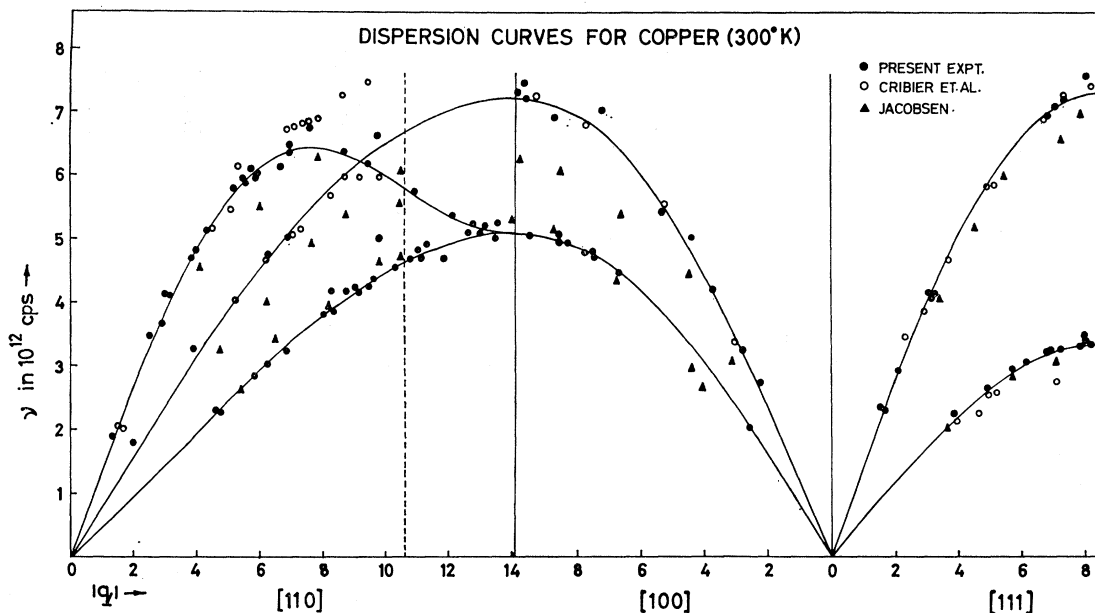


FIG. 2. The smooth curves represent the sixth-neighbor force model fitted to the present experimental data, and to the measured elastic constants.  $q$  is in units of  $\frac{1}{10} (2\pi/a)$ .

particularly near the zone boundaries on the  $[100]$  axis. The agreement is best for results along the  $[111]$  axis. On the whole, the x-ray results give frequencies which seem to be too low for the longitudinal modes. The agreement between the present results and those of Cribier *et al.* is better. However, along the  $[110]$  axis, the present results seem to indicate that the  $L$  and  $T_1$  modes cross over before the zone boundary, whereas the results of Cribier *et al.* indicate the opposite. It is to be noted that symmetry arguments indicate that these two branches must cross somewhere along the

$[110]$  axis, as at the point  $(2\pi/a)(1,1,0)$  ( $a$ =lattice constant) the  $L$   $[110]$  branch has to be degenerate with the  $T$   $[100]$  branch at a frequency of  $5.05 \times 10^{12}$  cps whereas the  $T_1$   $[110]$  branch has to be degenerate with the  $L$   $[100]$  branch at a frequency of  $7.2 \times 10^{12}$  cps. If the results of Cribier *et al.* for this axis were correct, the last (unmeasured) bit of their longitudinal branch would have to dip very steeply just before the zone boundary. The  $T$   $[111]$  branch as measured by these authors seems also to be slightly lower than in the present measurements.

TABLE II. Interpolated normal-mode frequencies in copper at 300°K for points along symmetry directions. ( $\nu$  in  $10^{12}$  cps, and  $\bar{q}$  in units of  $2\pi/a$ .)

$\bar{q}$	$(\bar{q},0,0)T$	Cu/Ni <sup>a</sup>	$(\bar{q},0,0)L$	Cu/Ni <sup>a</sup>		
0.2	1.57	1.29	2.31	1.35		
0.4	3.03	1.26	4.40	1.27		
0.6	4.18	1.22	5.95	1.23		
0.8	4.86	1.24	6.90	1.21		
1.0	5.05	1.24	7.20	1.19		
$\bar{q}$	$(\bar{q},\bar{q},\bar{q})T$	Cu/Ni	$(\bar{q},\bar{q},\bar{q})L$	Cu/Ni		
0.1	1.05	1.27	2.38	1.28		
0.2	1.99	1.24	4.55	1.23		
0.3	2.73	1.24	6.13	1.21		
0.4	3.20	1.26	7.05	1.21		
0.5	3.35	1.27	7.29	1.22		
$\bar{q}$	$(\bar{q},\bar{q},0)T_1$ <sup>b</sup>	Cu/Ni	$(\bar{q},\bar{q},0)T_2$ <sup>b</sup>	Cu/Ni	$(\bar{q},\bar{q},0)L$	Cu/Ni
0.2	1.32	1.48	2.25	1.23	3.62	1.23
0.4	2.77	1.31	4.35	1.26	5.98	1.21
0.6	3.99	1.25	5.90	1.16	6.38	1.20
0.75	4.61	...	6.67	1.13	5.78	1.26

<sup>a</sup> The ratio for corresponding frequencies in copper and nickel has been obtained using the values for nickel given in Ref. 11.

<sup>b</sup> The polarization vectors for the  $T_1$  and  $T_2$  modes propagating along the  $[110]$  axis are parallel to  $[1\bar{1}0]$  and  $[001]$ , respectively.

The lattice frequencies at some special values of  $\mathbf{q}$  as deduced by interpolation from the present results, using the fitted force-constant model, are given in Table II. For comparison, the table also shows the ratio of the frequencies in copper to the corresponding frequencies in nickel as determined by Birgeneau *et al.*<sup>11</sup> It may be seen that this ratio is fairly constant at about 1.25 for all frequencies. At low frequencies, the ratio is in general larger than at higher frequencies.

## ANALYSIS OF RESULTS

As is well known<sup>17</sup> the frequencies of a monatomic lattice are obtained from the solutions of the secular equation

$$|D_{\alpha\beta}(\mathbf{q}) - 4\pi^2 M \nu_j^2(\mathbf{q})| = 0, \quad [M = \text{Mass of ion}], \quad (4)$$

where the dynamical matrix  $D_{\alpha\beta}(\mathbf{q})$  may be expressed as a Fourier series,

$$D_{\alpha\beta}(\mathbf{q}) = -\sum_{\mathbf{l}} \phi_{\alpha\beta}(\mathbf{l}) \exp(i\mathbf{q} \cdot \mathbf{l}), \quad (5)$$

<sup>17</sup> M. Born and K. Huang, *The Dynamical Theory of Crystal Lattices* (Clarendon Press, Oxford, England, 1954).

where  $\mathbf{l}$  denotes a vector from the origin to another ion of the lattice and  $\phi_{\alpha\beta}(\mathbf{l})$  may be regarded as the force-constant matrix between the ion at  $\mathbf{l}$  and the origin ion. Strictly speaking, it is not possible to determine the  $\phi_{\alpha\beta}(\mathbf{l})$  from the measured lattice frequencies, without a knowledge of the polarization vectors as well.<sup>18</sup> However, in the absence of such data, the usual procedure has been to try to fit a small number of such parameters to the  $\nu_j(\mathbf{q})$  alone by postulating the  $\phi_{\alpha\beta}(\mathbf{l})$  to be zero after a stipulated number of neighbors. The number of such parameters that can then be determined from a knowledge of the lattice frequencies in the the (001) and (110) symmetry planes of a cubic lattice has been discussed by Squires.<sup>19</sup> He has shown that from a knowledge of the frequencies in the planes, all the force constants for a model extending up to at least 15th neighbors can be determined. It should be noted, however, that if one does not restrict oneself to a finite neighbor model, can obtain different sets of such "force constants" which will reproduce the same lattice frequencies, but with different polarization vectors.<sup>15</sup> The extent to which we can believe the fitted parameters for the finite-neighbor model chosen will therefore be somewhat influenced by the extent to which we believe in the finite range of forces between the atoms in the lattice, even if a "good fit" is obtained to the experimental results. As discussed below, the behavior of the parameters under the fitting process in the present case was more consistent with the existence of long-range forces.

The method of least-squares fitting of force constants to the dispersion relations for cubic crystals has been discussed in detail by Squires.<sup>20</sup> The process is carried out for increasing numbers of neighbors in turn, using the values of the preceding fit as initial estimates for the force constants at each stage. The force constants are at all stages subjected to three linear constraints imposed by the three measured elastic constants as mentioned above.

It was found that as higher terms in the series for  $D_{\alpha\beta}(\mathbf{q})$  were included, the fit improved rapidly up to a third-neighbor model and thereafter much more slowly. The process was continued up to sixth neighbors. Unfortunately, the individual values of the smaller force constants (involving second and further neighbors) did not show convergent behavior as the higher terms were included, but instead showed fluctuations of their own order of magnitude or greater. This is similar to the behavior reported by Squires<sup>20</sup> in an analysis of the dispersion relations in aluminum. This may be partly due to the fact that, except along symmetry direction of the reciprocal lattice, the functions  $\nu_j^2(\mathbf{q})$  are not expressible as a series of orthogonal functions, with the parameters as coefficients of successive terms.<sup>18</sup> However, the result does show that a force-constant model involving a small

TABLE III. Force constants for best fitted 6th-neighbor model.<sup>a</sup>

$$\phi \equiv - \begin{pmatrix} \alpha_1 & \beta_3 & \beta_2 \\ \beta_3 & \alpha_2 & \beta_1 \\ \beta_2 & \beta_1 & \alpha_3 \end{pmatrix} \quad \text{Units are in dynes/cm.}$$

Neighbor location	Force constants
First (1,1,0)	$\alpha_1 = 13478$ $\alpha_3 = -1215$ $\beta_3 = 14982$
Second (2,0,0)	$\alpha_1 = 18$ $\alpha_2 = -48$
Third (2,1,1)	$\alpha_1 = 507$ $\alpha_2 = 239$ $\beta_1 = 159$
Fourth (2,2,0)	$\beta_2 = 378$ $\alpha_1 = 267$ $\alpha_3 = -32$
Fifth (3,1,0)	$\beta_3 = -36$ $\alpha_1 = -110$ $\alpha_2 = -203$
Sixth (2,2,2)	$\alpha_3 = 37$ $\beta_3 = 18$ $\alpha_1 = -157$ $\beta_1 = -58$

<sup>a</sup> The force constants not listed may be obtained from the above using symmetry arguments.

number of neighbors is probably not valid. The values of the nearest-neighbor force constants, on the other hand, were always found to be very much larger than those involving further neighbors, at all stages of the fitting process. Qualitatively, one can at least say that this reflects the dominance of the exchange or overlap repulsion between neighboring ion cores, which is known to be large in copper.<sup>21</sup>

For the above reasons, the actual numerical values of the final sixth-neighbor model cannot be ascribed any physical significance, but can be considered rather as providing a useful interpolation formula for the dispersion relations, from which calculations of quantities such as the frequency distribution function or the second-order resolution corrections could be made. Figure 2 shows that the interpolation formula is very good and is within the limits of experimental accuracy. The force constants are listed in Table III.

Using the above sixth-neighbor force model, a frequency distribution function  $g(\nu)$  was constructed by sampling the eigenvalues of the dynamical matrix at a grid of 6281 points equally spaced inside the elementary  $1/48$  volume of the first Brillouin zone. The  $\mathbf{q}$  values at which the frequencies were calculated were then multiplied by the appropriate factor to give all such equivalent points in the Brillouin zone. The frequency interval chosen to collect a sampling of the number of frequencies in the interval was  $0.035 \times 10^{12}$  cps and the histogram thus obtained was smoothed out to form a continuous curve. This is shown in Fig. 3 which also indicates the positions of some of the critical points<sup>22</sup> as obtained from the appropriate points on the dispersion curves. It may

<sup>18</sup> A. J. E. Foreman and W. M. Lomer, Proc. Phys. Soc. (London) **B70**, 1143 (1957).

<sup>19</sup> G. L. Squires, Arkiv. Fysik **25**, 21 (1963).

<sup>20</sup> G. L. Squires, Arkiv. Fysik **26**, 223 (1964).

<sup>21</sup> N. F. Mott and H. Jones, *The Theory of the Properties of Metals and Alloys* (Oxford University Press, New York, 1936), p. 144.

<sup>22</sup> L. Van Hove, Phys. Rev. **89**, 1189 (1953).

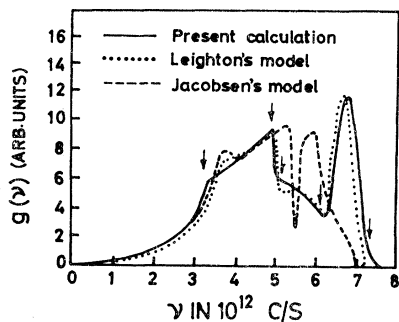


FIG. 3. Frequency distribution functions for copper at 300°K. The arrows indicate the positions of some of the critical points.

be seen that the  $g(\nu)$  obtained is appreciably different from that obtained by Jacobsen<sup>9</sup> by fitting a third-neighbor model to his measured dispersion curves, especially on the high-frequency side. It is very similar on the other hand to that obtained from a simple two-constant model postulated by Leighton.<sup>1</sup> Figure 4 shows that the temperature variation of the Debye temperatures obtained from the above  $g(\nu)$  is in very good agreement with experiment<sup>23,24</sup> except at very low temperatures. The discrepancy at low temperatures is due to the model having been fitted to the dispersion relation at room temperature. At very low temperatures, the elastic moduli determine the Debye temperature, and are about 5% different from those at room temperature.<sup>16</sup> Table IV shows that the calculation of the Debye-Waller factor for copper at different temperatures using the above  $g(\nu)$  is also in good agreement with experiment. The experimental and other theoretical values in that table are listed by De Wames *et al.*<sup>25</sup> and include calculations based on their axially symmetric (A.S.) force model.<sup>6</sup> It is to be noted that the sixth-neighbor "best fit" force constants used in our calculations do not all satisfy the A.S. condition. However, for the nearest-neighbor force constants, the A.S. condi-

TABLE IV. Temperature variation of the Debye-Waller factor for copper. All values except those from the present calculations taken from Ref. (25).  $C(T)$ , defined by  $e^{-2W} = e^{-h^2 K^2 C(T)/2M}$ , is in units of  $10^2 \text{ eV}^{-1}$ .

$T(^{\circ}\text{K})$	Exptl. (Flinn <i>et al.</i> )	Present calculation	Model (a) <sup>a</sup>	Model (b) <sup>b</sup>	Model (c) <sup>c</sup>	Debye model
4	$0.544 \pm 0.02$	0.555	0.552	0.579	0.570	0.520
20	$0.588 \pm 0.02$	0.565	0.566	0.593	0.582	0.532
80	$0.755 \pm 0.04$	0.754	0.762	0.808	0.779	0.697
300	$2.17 \pm 0.14$	2.10	2.10	2.29	2.18	1.93
400	$3.14 \pm 0.25$	2.76	2.77	3.02	2.87	2.50

<sup>a</sup> Model (a)—"2 parameter" model due to Leighton (Ref. 1).

<sup>b</sup> Model (b)—Model due to Jacobsen (Ref. 5).

<sup>c</sup> Model (c)—Axially Symmetric model due to De Wames *et al.* (Ref. 25).

<sup>23</sup> W. C. Overton, Jr., *VIIIth International Conference on Low Temperature Physics* (University of Toronto Press, Toronto, 1960), p. 677 and references therein.

<sup>24</sup> W. F. Giaque and P. F. Meads, *J. Am. Chem. Soc.* **63**, 1897 (1941).

<sup>25</sup> R. E. De Wames, T. Wolfram, and G. W. Lehman, *Phys. Rev.* **131**, 528 (1963).

tion is satisfied to within 3% and is in fact always well satisfied for all stages of the fitting process beyond third neighbors. Because of the indeterminacy of the smaller force constants as discussed earlier, it is possible that a good fit may also be obtained by constraining the force constants from the start to be completely axially symmetric. This has not been done for the present results. Again, such a model would certainly have to go out to at least third neighbors to give a good fit.

### COMPARISON WITH THEORY

Recently, there have been several theoretical treatments of the lattice dynamics of metals, which start from more basic principles than the force-constant approach discussed above.<sup>5,26,27</sup> See, for example, the recent review article by Cochran.<sup>28</sup>

In particular, Toya<sup>29</sup> has applied his theory to a calculation of the dispersion relations in copper. The dynamical matrix is conventionally expressed as a sum of terms due to three different types of interactions,

$$D_{\alpha\beta}(\mathbf{q}) = C_{\alpha\beta}(\mathbf{q}) + R_{\alpha\beta}(\mathbf{q}) + E_{\alpha\beta}(\mathbf{q}), \quad (6)$$

where  $C_{\alpha\beta}(\mathbf{q})$  is the contribution from electrostatic forces between ions regarded as point charges, such as has been evaluated by Kellerman<sup>30</sup>;  $R_{\alpha\beta}(\mathbf{q})$  is the contribution from direct overlap or exchange repulsions between ion cores; and  $E_{\alpha\beta}(\mathbf{q})$  is the contribution of the conduction electrons, representing the effective ion-electron-ion interaction.

We shall first discuss the second term above. As stated in the Introduction, the core-overlap interaction parameters are known to be large for the noble metals,<sup>21</sup> (as is also evident from the results of the force-constant fitting procedure described above), but are not very well known. Fuchs<sup>31,32</sup> attempted a quantum-mechanical calculation of the overlap interaction between two

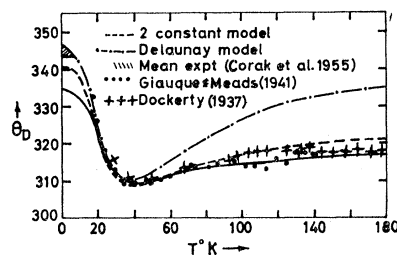


FIG. 4. Temperature variation of the Debye temperature for copper. The experimental points, and the calculations, other than the present one, are taken from Ref. 23. The full line denotes the present calculation.

<sup>26</sup> L. J. Sham, *Proc. Roy. Soc. (London)* **A283**, 33 (1965).

<sup>27</sup> W. A. Harrison, *Phys. Rev.* **129**, 2503 (1963); **129**, 2512 (1963).

<sup>28</sup> W. Cochran, *Inelastic Scattering of Neutrons* (International Atomic Energy Agency, Vienna, 1965), Vol. I, p. 3.

<sup>29</sup> T. Toya, *J. Res. Inst. Catalys. Hokkaido Univ.* **9**, 178 (1961).

<sup>30</sup> E. W. Kellerman, *Phil. Trans. Roy. Soc. London* **238**, 513 (1940).

<sup>31</sup> K. Fuchs, *Proc. Roy. Soc. (London)* **A151**, 585 (1935).

<sup>32</sup> K. Fuchs, *Proc. Roy. Soc. (London)* **A153**, 622 (1935).

TABLE V. Values of the core-overlap interaction parameters in copper as obtained by different methods.

		$A$ (eV)	$\rho$
Fuchs <sup>a</sup>		0.042	16.47
Huntington <sup>b</sup>	(a)	0.053	13.9
	(b)	0.038	17.2
Mann & Seeger <sup>b</sup>	(a)	0.011	26.9
	(b)	0.041	16.6
	(c)	0.077	13.6
	(d)	0.075	12.55
	(e)	0.0910	12.10
	(f)	0.1081	11.75
Toya		0.120	11.50
White		0.185	11.47
Present calculation		0.017	24.11
Thompson		0.045	13.0

<sup>a</sup> Fuchs did not assume the Born-Mayer form for  $\phi^R(r)$ . His results have been converted into equivalent Born-Mayer parameters.

<sup>b</sup> The values given are quoted in Ref. 35. Values (a), (b), and (c) of Mann and Seeger were obtained by fitting to the room-temperature shear moduli by making different assumptions about the electronic contributions. Values (d), (e), and (f) were similarly obtained by fitting to the pressure variation of the shear moduli with similar assumptions.

copper ions, and showed that good agreement was obtained with the measured elastic moduli, if one assumed that the conduction electrons did not contribute at all to the shear moduli. However, it will be shown that for a metal with appreciable band gaps, such as copper, this assumption is not valid.

The core-overlap interaction is usually represented in the Born-Mayer form, as a pair-potential function between neighboring ion-cores, by

$$\phi^R(r) = A \exp\{\rho(r_1 - r)/r_1\} \quad (7)$$

$[r_1 = \text{nearest-neighbor distance}]$ .

Various attempts<sup>33-35</sup> have been made to estimate  $A$  and  $\rho$  from the values of the measured elastic moduli, or from other data, such as the variation of the compressibility with pressure. Mann and Seeger<sup>34</sup> have given a critical review of the values of these parameters. In each case, various assumptions have been made about the value of the electronic contribution to the elastic moduli. These assumptions cannot be justified theoretically to better than an order of magnitude. It is not surprising therefore that there is not very good agreement between the values obtained by the different methods. Table V

TABLE VI. Relevant constants for copper.

$a$	3.615 Å
$r_s$	1.413 Å
$D/D_0$	0.875
$m^*$	1.0 in units of free-electron mass
$N$	$8.468 \times 10^{22} \text{ cm}^{-3}$
$k_f$	$1.358 \text{ Å}^{-1}$
$C$	1.37
$E_F$	7.04 eV

<sup>33</sup> H. B. Huntington, Phys. Rev. **91**, 1092 (1953).

<sup>34</sup> K. Kambe, Phys. Rev. **99**, 419 (1955).

<sup>35</sup> E. Mann and A. Seeger, J. Phys. Chem. Solids **12**, 314 (1960).

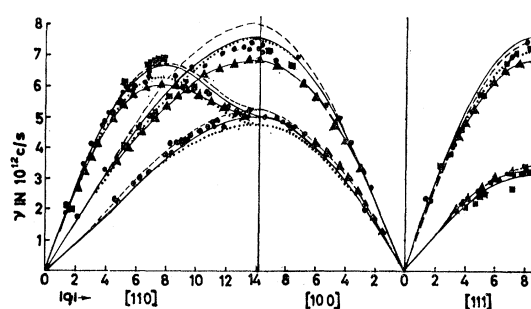


FIG. 5. Comparison of the theoretical calculations of the dispersion curves in copper along the symmetry directions with the present data (solid circles) and those of Cribier *et al.* (squares). The full line represents the present calculation assuming central core-overlap forces. The dotted line represents a similar calculation assuming general first-neighbor core-overlap forces. The dashed line represents calculations based on White's model, and the line  $\blacktriangle-\blacktriangle-\blacktriangle$  represents Toya's model. For the  $T_1[110]$  branch, Toya's curve is indistinguishable from the full line, while for the  $T[111]$  branch, the dotted line coincides with the full line. For the  $T[100]$  branch, Toya's curve coincides with the full line near the zone boundary.

lists the different values for  $A$  and  $\rho$  as given in the literature. Also shown are values obtained from recent experiments by Thompson<sup>36</sup> on the tunnelling of high-energy copper ions through a copper lattice. These provide in principle a direct observation of the interaction between two copper ions. It is to be noted that, whether the core-overlap interaction is really given by an expression of the form (7) or not,  $A$  and  $\rho$  merely provide another way of expressing the two basic core-overlap parameters that enter into the lattice dynamics, namely,

$$\left. \frac{\phi'(r)}{r} \right|_{r=r_1} \quad \text{and} \quad \phi''(r)|_{r=r_1}.$$

Table VI lists some of the relevant constants for copper.

The procedure adopted by Toya was to use his theory to calculate  $E_{\alpha\beta}(\mathbf{q})$  and leave  $A$  and  $\rho$  as two adjustable parameters to be obtained by fitting the lattice frequencies for the  $L[111]$  and  $T[111]$  modes at the zone boundary, as measured by Jacobsen.<sup>9</sup> Figure 5 shows the dispersion curves calculated by Toya along the symmetry directions of the lattice. It may be seen that whilst agreement with the experimentally observed transverse modes is good, the calculated frequencies for the longitudinal modes and the  $T_1[110]$  mode tend to be too low. This is possibly due to the fact that the core-overlap parameters  $A$  and  $\rho$  were fitted to Jacobsen's results which are too low in comparison with the neutron-scattering data, especially for the longitudinal mode. Recently Toya<sup>37</sup> has refitted  $A$  and  $\rho$  for copper

<sup>36</sup> M. W. Thompson, Atomic Energy Research Establishment (Great Britain) Harwell Report, 1964 (unpublished). See also R. S. Nelson and M. W. Thompson, Phil. Mag. **8**, 1677 (1963).

<sup>37</sup> T. Toya, *Inelastic Scattering of Neutrons in Solids and Liquids* (International Atomic Energy Agency, Vienna, 1965), Vol. I, p. 25.



to the present neutron results and obtained much better agreement for the longitudinal modes as well. However, it should be noted, that, using Toya's calculated values for  $E_{\alpha\beta}(\mathbf{q})$  it is intrinsically impossible to find  $A$  and  $\rho$  to fit all three measured elastic constants, without modifying any parameter in Toya's theory. Since, in principle, Toya's theory provides a more accurate method of calculating the electronic contribution to the elastic constants than previous methods, it was decided to attempt to modify a single parameter in Toya's expression for  $E_{\alpha\beta}(\mathbf{q})$  so as to obtain an  $A$  and  $\rho$  to fit all three elastic moduli.

In order to facilitate the discussion afterwards, we shall first consider the general expression for  $E_{\alpha\beta}(\mathbf{q})$  which is valid even for metals which are not "free-electron-like." Such an expression has been derived by Sham,<sup>26</sup> and, within the "local pseudopotential ap-

proximation," it is

$$E_{\alpha\beta}(\mathbf{q}) = (4\pi N e^2/3)\delta_{\alpha\beta} + \sum_{\mathbf{H}, \mathbf{H}'} \phi_{\alpha\beta}(\mathbf{q}, \mathbf{H}, \mathbf{H}') - \sum_{\mathbf{H}, \mathbf{H}' \neq 0} \phi_{\alpha\beta}(\mathbf{0}, \mathbf{H}, \mathbf{H}'), \quad (8)$$

( $N$  = number of conduction electrons per unit volume;  $\mathbf{H}, \mathbf{H}'$  denote reciprocal lattice vectors), where the first term is the effect of the uniform part of the conduction-electron charge density, and

$$\phi_{\alpha\beta}(\mathbf{q}, \mathbf{H}, \mathbf{H}') = [(4\pi N e^2/|\mathbf{q} + \mathbf{H}|^2)\{1 - f(\mathbf{q} + \mathbf{H})\}]^{-1} \times [\epsilon^{-1}(\mathbf{q} + \mathbf{H}, \mathbf{q} + \mathbf{H}') - \delta_{\mathbf{H}\mathbf{H}'}][(\mathbf{q} + \mathbf{H})_{\alpha}(\mathbf{q} + \mathbf{H}')_{\beta}] \times U^*(\mathbf{q} + \mathbf{H})U(\mathbf{q} + \mathbf{H}'), \quad (9)$$

where  $U(\mathbf{K})$  is the Fourier Transform of the "bare" ionic pseudo-potential, and the dielectric matrix is defined by

$$\epsilon(\mathbf{q} + \mathbf{H}, \mathbf{q} + \mathbf{H}') = \delta_{\mathbf{H}\mathbf{H}'} - \frac{4\pi N e^2}{|\mathbf{q} + \mathbf{H}|^2} [1 - f(\mathbf{q} + \mathbf{H})] \sum_{\mathbf{k}, \mathbf{H}''} \frac{n(\mathbf{k}) - n(\mathbf{k} + \mathbf{q} + \mathbf{H}'')}{E(\mathbf{k}) - E(\mathbf{k} + \mathbf{q} + \mathbf{H}'')} \times \langle \mathbf{k} | e^{-i(\mathbf{q} + \mathbf{H}) \cdot \mathbf{r}} | \mathbf{k} + \mathbf{q} + \mathbf{H}'' \rangle \langle \mathbf{k} + \mathbf{q} + \mathbf{H}'' | e^{i(\mathbf{q} + \mathbf{H}') \cdot \mathbf{r}} | \mathbf{k} \rangle. \quad (10)$$

$E(\mathbf{k})$  refers to the single-electron energy and  $n(\mathbf{k})$  to the occupation number of state  $|\mathbf{k}\rangle$ . The states  $|\mathbf{k}\rangle$  are taken to be the "smooth" parts of the electron wave function, or a linear combination of OPW's. In Eqs. (9) and (10),  $f(\mathbf{q} + \mathbf{H})$  is a function that approximately takes into account exchange and correlation effects. Sham<sup>26</sup> takes it to be

$$f(\mathbf{q} + \mathbf{H}) = \frac{1}{2} \frac{|\mathbf{q} + \mathbf{H}|^2}{|\mathbf{q} + \mathbf{H}|^2 + k_f^2 + k_s^2}, \quad (11)$$

( $k_f$  = Fermi wave vector and  $k_s$  = the Fermi-Thomas screening vector) which tends to one-half for large  $|\mathbf{q} + \mathbf{H}|$ . The last term in (8) arises from the "intrinsic two-phonon process"<sup>26</sup> and can be shown to be of the right magnitude to make the frequencies tend to zero as  $\mathbf{q} \rightarrow 0$ .

Unfortunately, if the "smooth" parts  $|\mathbf{k}\rangle$  of the electron wave function  $\psi_{\mathbf{k}}$  have to be represented by more than a single plane wave, and the  $E(\mathbf{k})$  are not free-electron-like energies, then the calculation of  $\epsilon(\mathbf{q} + \mathbf{H}, \mathbf{q} + \mathbf{H}')$  becomes extremely complicated. Toya's theory is equivalent to invoking the single orthogonalized-plane-wave approximation. In this approximation, only terms with  $\mathbf{H} = \mathbf{H}'$  survive in Eqs. (9) and (10). Toya further takes exchange and correlation into account by choosing

$$f(\mathbf{q} + \mathbf{H}) = \frac{C|\mathbf{q} + \mathbf{H}|^2}{4k_f^2} [C|\mathbf{q} + \mathbf{H}|^2 \leq 4k_f^2], \quad (12a)$$

where  $C$  is a constant. And for  $C|\mathbf{q} + \mathbf{H}|^2 > 4k_f^2$ , Toya puts

$$f(\mathbf{q} + \mathbf{H}) = 1. \quad (12b)$$

Thus the large wave-vector limits of (11) and (12) are different.

To further allow for the effect of exchange and correlation on the  $E(\mathbf{k})$ , Toya multiplies  $[E(\mathbf{k}) - E(\mathbf{k} + \mathbf{q} + \mathbf{H}'')]^{-1}$  in Eq. (10) by a factor  $D/D_0$  representing the ratio of the density of states at the Fermi surface with and without such effects. Finally, as an analytic expression for the Fourier transform of the pseudopotential Toya adopts the expression originally derived by Bardeen<sup>33</sup> using a different method.

$$U(\mathbf{K}) = -[(4\pi N e^2/K^2) + U_0]g(Kr_s), \quad (13)$$

where  $r_s$  = atomic cell radius, and

$$g(x) = 3(\sin x - x \cos x)/x^3 \quad (14)$$

and  $U_0$  is a constant denoting the depth of the square-well potential in the atomic cell, which approximates the sum of the Wigner-Seitz potential and the potential due to a uniform density of conduction electrons in the Wigner-Seitz cell. By analogy with Bardeen's original result, it may be represented by

$$U_0 = V(r_s) - E_0, \quad (15)$$

where  $V(r_s)$  is the Hartree-Fock (H.F.) potential at the surface of the atomic sphere and  $E_0$  is the H.F. energy of the state  $\mathbf{k} = 0$ . Toya takes as the value of this parameter 4.05 eV on the basis of earlier band-structure calculations for copper. For our calculation, we have regarded this as the most uncertain parameter in the theory.

It should be noted that the last term in Eq. (8)

<sup>33</sup> J. Bardeen, Phys. Rev. **52**, 683 (1937).

vanishes in the single OPW or "free-electron-like" approximation. This is consistent with the fact that such an approximation implies vanishing band gaps and hence requires  $U(\mathbf{K})$  to vanish at all reciprocal lattice points except the origin. Hence Toya adds a correction term to  $g(Kr_s)$  in Eq. (13), so that  $U(\mathbf{K})$  approximately vanishes for  $\mathbf{K}=(2\pi/a)(1,1,1)$  and  $\mathbf{K}=(2\pi/a)(2,0,0)$ , although this makes  $U(\mathbf{K})$  for larger values of  $K$  unreliable. However, he then cuts off the sum in (8) for  $|\mathbf{q}+\mathbf{H}| > (2\pi/a)\sqrt{3}$ . In our present calculation, however, the correction terms to  $g(Kr_s)$  have not been added, and the sum in (8) has been taken up to  $|\mathbf{K}|=(2\pi/a)(11)^{1/2}$ , to approximately allow for the fact that copper has finite band gaps. The last terms in (8) are now non-vanishing and have also been added to give the correct limit at  $\mathbf{q}=0$ . Nevertheless, when calculating the expression (9), single plane-wave states were assumed, and Toya's expression adopted.

We obtain from Eqs. (8)-(10) and (12)-(14),

$$E_{\alpha\beta}(\mathbf{q}) = \frac{4\pi N e^2}{3} \delta_{\alpha\beta} - 4\pi N e^2 \sum_{\mathbf{H}} \frac{(\mathbf{q}+\mathbf{H})_{\alpha}(\mathbf{q}+\mathbf{H})_{\beta}}{|\mathbf{q}+\mathbf{H}|^2} \\ \times \{G(t)\}^2 \{F(t)\}^{-1} f(t) + 4\pi N e^2 \sum_{\mathbf{H} \neq 0} \frac{H_{\alpha} H_{\beta}}{H^2} \\ \times \{G(t_H)\}^2 \{F(t_H)\}^{-1} f(t_H), \quad (16)$$

where

$$\mathbf{t} = (\mathbf{q}+\mathbf{H})/2k_f; \quad \mathbf{t}_H = \mathbf{H}/2k_f,$$

and

$$G(t) = \left\{ 1 + U_0 \frac{3\pi}{e^2 k_f} t^2 \right\} g(2k_f r_s t), \\ f(t) = \frac{1-t^2}{4t} \ln \left| \frac{1+t}{1-t} \right|, \\ F(t) = \frac{D_0 \pi \hbar^2 k_f}{D m^* e^2} t^2 + (1 - C t^2) f(t), \quad [C t^2 \leq 1] \\ F(t) = \frac{D_0 \pi \hbar^2 k_f}{D m^* e^2} t^2, \quad [C t^2 > 1]. \quad (17)$$

By expanding in the long-wavelength limit we may evaluate from Eq. (16) the expressions for the electronic contributions to the elastic moduli, which we write in the form,

$$(c_{11} + 2c_{44})^E = -\frac{4\pi N^2 e^2}{3} \frac{1}{8k_f^2} \\ \times \left[ \left( 6C - 6 \frac{D_0 \pi \hbar^2 k_f}{D m^* e^2} - \frac{24r_s^2 k_f^2}{5} + \frac{36\pi U_0}{e^2 k_f} \right) \right. \\ \left. + \sum_{\mathbf{H} \neq 0} \{S''(t_H) + 2S'(t_H)/t_H\} \right], \quad (18a)$$

$$(c_{11} - c_{12})^E = -\frac{4\pi N^2 e^2}{8k_f^2} \sum_{\mathbf{H} \neq 0} \left[ (4H_{\alpha}^2 - 2H_{\beta}^2) Y(t_H) \right. \\ \left. + (H_{\alpha}^4 - H_{\alpha}^2 H_{\beta}^2) Z(t_H) \right], \quad (18b)$$

$$c_{44}^E = -\frac{4\pi N^2 e^2}{8k_f^2} \sum_{\mathbf{H} \neq 0} \left[ \frac{2S(t_H)}{t_H^2} \right. \\ \left. + 2(H_{\alpha}^2 + H_{\beta}^2) Y(t_H) + 2H_{\alpha}^2 H_{\beta}^2 Z(t_H) \right], \quad (18c)$$

where

$$S(t) = \{G(t)\}^2 \{F(t)\}^{-1} f(t), \\ Y(t) = \frac{1}{4k_f^2} \left\{ \frac{S'(t)}{t^3} - \frac{2S(t)}{t^4} \right\}, \\ Z(t) = \frac{1}{16k_f^4} \left\{ \frac{S''(t)}{t^4} - \frac{5S'(t)}{t^5} + \frac{8S(t)}{t^6} \right\},$$

$\alpha, \beta$  denote any two different Cartesian components, and the primes denote differentiation with respect to  $t$ . From Eqs. (18b) and (18c) it may be seen that only the umklapp processes from  $\mathbf{H} \neq 0$  contribute to the shear moduli. This contribution will only vanish in a genuinely free-electron-like approximation, as then  $U(\mathbf{H})=0$  implies  $S(t_H)=0$  for  $\mathbf{H} \neq 0$ . For a metal with appreciable band gaps, however, the conduction electrons will certainly contribute to the shear moduli.

The Coulomb or electrostatic contribution to these moduli has been given by Fuchs<sup>32</sup> as

$$(C_{11} - C_{12})^C = 0.2115 N e^2 / 2a, \\ (C_{44})^C = 0.9479 N e^2 / 2a,$$

while  $(C_{11} + 2c_{44})^C = 0$  because the electrostatic interaction does not contribute to the trace of the dynamical matrix.<sup>18</sup> Using the above values, the contributions of the core-overlap interactions to the three elastic moduli were obtained by subtracting the electronic and Coulomb parts from the measured elastic moduli (see Table VII). These three quantities cannot in general be solved in terms of the two parameters  $A$  and  $\rho$ . By regarding  $U_0$  as a variable parameter, it was found possible to fit all three elastic moduli with central core-overlap forces if  $U_0=0.5$  eV. We may compare this with estimates of the quantity  $[V(r_s) - E_0]$  [see Eq. (15)] obtained from recent band-structure calculations on copper<sup>39,40</sup> as listed in Table VIII. The value of  $A$  and  $\rho$  obtained from the above fit to the elastic constants are listed in Table V.

Dispersion curves along the symmetry axes calculated from Eqs. (6) and (8) using the above parameters are shown in Fig. 5. The fit along the transverse branches is very good. The longitudinal branches tend to be a

<sup>39</sup> G. A. Burdick, Phys. Rev. **129**, 138 (1963).

<sup>40</sup> B. Segall, Phys. Rev. **125**, 109 (1962).

TABLE VII. Elastic constants of copper and theoretical estimates of various contributions to shear moduli. Units are in  $10^{11}$  dyn/cm<sup>2</sup>.

20°K <sup>(16)</sup>		Room temperature <sup>(16)</sup>		
$C_{11}$	17.618		16.839	
$C_{12}$	12.492		12.142	
$C_{44}$	8.173		7.539	
$C_{11}-C_{12}$		Fuchs	Present calculation <sup>a</sup>	White <sup>a</sup>
Core overlap		4.498	4.017	6.418
Electronic		0.0	0.113	-2.373
Coulomb		0.573	0.573	0.573
Total		5.071	4.703	4.618
Exptl. (Room temp.)		4.7		
Exptl. (20°K)		5.13		
$C_{44}$		Fuchs	Present calculation <sup>a</sup>	White <sup>a</sup>
Core overlap		6.266	5.345	12.17
Electronic		0.0	-0.375	-7.32
Coulomb		2.57	2.57	2.57
Total		8.836	7.54	7.42
Exptl. (Room temp.)		7.54		
Exptl. (20°K)		8.17		

<sup>a</sup> Note: Both White's model and the present calculations have been fitted to the elastic moduli at room temperature.

little too high near the zone boundaries, the maximum discrepancy being about 4%. Dispersion curves calculated for off-symmetry directions also show very similar agreement with the experimental results.

It is interesting to compare the value for  $\phi'(r)|_{r=r_1}$  [where  $\phi(r)$  is the core-overlap potential defined in (7), and  $r_1$  is the distance between neighboring ions] obtained above with that obtained by applying the condition for lattice equilibrium. In the "free-electron" approximation, the expression for  $dE_c/dr_s$  (where  $E_c$  is the cohesive energy) has been evaluated by Toya.<sup>29</sup> Equating this to zero, we get for  $\phi'(r_1)$  the value of  $-0.2646 \times 10^4$  dyn/cm. The value calculated above is  $-0.1034 \times 10^4$  dyn/cm.

An attempt was also made to use a general (i.e., non-central) core-overlap interaction model keeping  $U_0$  fixed at the value chosen by Toya. We then have three first-neighbor force parameters to describe this interaction and these can be solved in terms of the measured elastic moduli and the calculated electronic and Coulomb contributions. The dispersion curves calculated using this model are shown as the dotted curve in Fig. 5. It is seen that agreement with experiment is generally worse than in the case of central core-overlap forces. This is borne out by the fact that the least-squares-fitted first-neighbor force constants always nearly satisfied the axially symmetric condition.

TABLE VIII. Various estimates of  $U_0 = V(r_s) - E_0$  for copper.

	$V(r_s) - E_0$
Present calculation	0.5 eV
Burdick (39)	1.361 eV
Segall (40)	-0.871 eV
Chodorow (quoted by Burdick)	1.414 eV

White<sup>41</sup> has also attempted to calculate directly the interatomic force constants in copper, using an approach rather different from that of Toya. He has calculated the force constants out to third nearest neighbors and fitted the core-overlap interactions to the elastic constants. His values for  $A$  and  $\rho$  (given in Table V) seem however considerably larger than all other values obtained for these parameters by other methods. Dispersion curves calculated from his theory are also shown in Fig. 5.

## SUMMARY AND DISCUSSION

An interpolation formula for the dispersion relations in copper at room temperature has been obtained by making a least-squares fit of a sixth-neighbor interatomic-force-constant model to the neutron-scattering results. However, because of the large variation of the parameters with the introduction of increasing neighbors, the values obtained for these cannot in themselves be ascribed any physical significance, beyond showing that (a) nearest-neighbor interactions dominate and that (b) the forces extend out to at least third neighbors and probably up to sixth neighbors.

The results have been compared with calculations based on Toya's treatment (with a few minor modifications) of the electron-phonon interaction in monovalent metals, which is equivalent to invoking the "free-electron-like" approximation for the electron wave functions, as discussed above. The values of the three most uncertain parameters in the theory, representing the depth of the pseudopotential-well due to the ions, and the two core-overlap interaction parameters have been obtained by fitting the theoretical expressions for the frequencies in the long-wavelength limit to those obtained from the measured elastic constants. The value of  $U_0$  thus obtained is not inconsistent with estimates obtained from recent band-structure calculations on copper,<sup>39,40</sup> although the values of  $U(\mathbf{K})$  derived from it using Bardeen's expression are not consistent with the band structure, as discussed below. The values obtained for the core-interaction parameters are not very different from other estimates of these parameters. Phonon-dispersion curves calculated from these parameters show fairly good quantitative agreement with the experimental results, especially for the transverse modes. It is possible that better agreement with the longitudinal modes might be obtained by a more accurate estimation of the exchange and correlation effects, for instance by replacing  $f(\mathbf{q}+\mathbf{H})$  as given in (12) by the expression (11), or by replacing the electron mass by an effective mass  $m^*$  and the electronic and ionic charges by  $e^*$  to allow for the fact that the "core part" of the conduction-electron wave function behaves like the core charge distributions.

However, the most serious drawback of the above treatment as applied to copper is due to the fact that it

<sup>41</sup> H. C. White, Phys. Rev. **112**, 1092 (1958).

is unlikely that single plane waves (or OPW's) can adequately represent even the "smooth" part of the electron wave functions. This is indicated by the band-structure calculations for this metal referred to above<sup>39,40</sup> and measurements of the Fermi surface<sup>42</sup> (see for instance, Ziman<sup>43</sup>). This is related to the fact that the Fourier transform of the (screened) ionic pseudopotential  $U_s(\mathbf{H})$  is large for at least the reciprocal lattice points  $(2\pi/a)(1,1,0)$  and  $(2\pi/a)(2,0,0)$  resulting in fairly large band gaps ( $\sim 2$  eV) at these points. On the other hand,  $U_s(\mathbf{H})$  as calculated from Eq. (13), with  $U_0$  as chosen above, and using the dielectric function of a free-electron gas, gives values which are much too small in comparison ( $\sim 0.1$  eV). (This is also true for  $U_0=4.05$  eV as taken by Toya.) Thus there is a basic inconsistency between the form of the pseudopotential used to calculate the electron-phonon interaction, and that used to calculate the band structure. This difficulty has been previously pointed out by Sham and Ziman.<sup>12</sup>

If one considers the electron-phonon interaction as a scattering process, in the manner suggested by Sham and Ziman, one can argue that a partial effect of the "multiphonon" terms would be to multiply the effective electron-phonon matrix element by a Debye-Waller factor. However, for the reciprocal lattice points considered, multiplication of the  $U_s(\mathbf{H})$  consistent with the band structure by such a factor does not reduce it to anything like the value calculated above. It may be argued that fitting parameters to the elastic constants as described above is not very reliable. As in the long-wavelength limit, the electronic contributions to the frequencies will depend strongly on the electronic states near the Fermi surface [see Eq. (10)] which are particularly non-free-electron like. However, it is still true that any accurate theory of the dispersion relation in copper must give results that are valid in this region too. Thus it seems necessary to evaluate the expressions (9) and (10) more accurately using states  $|\mathbf{k}\rangle$  and energies  $E(\mathbf{k})$  and a pseudopotential  $U(\mathbf{K})$  which are more consistent with the band structure of the metal. It is to be noted that, as pointed out by Cochran,<sup>28</sup> according to Eqs. (6)–(10) the above theory gives rise to an "axially symmetric" model of the effective force constants between ions, of the type proposed by Lehman *et al.*,<sup>6</sup> provided one neglects the off-diagonal elements of the

dielectric matrix  $\epsilon(\mathbf{q}+\mathbf{H}, \mathbf{q}+\mathbf{H}')$ , as is the case in the "free-electron" approximation. In fact, if one casts Eqs. (6) and (16) into the "force-constant" form, one obtains from the above calculations axially-symmetric force-constants which become negligible beyond fifth neighbors, owing to cancellation of the Coulomb and electronic contribution at large distances. Thus a test for axial symmetry in the experimental force constants could in principle indicate whether the off-diagonal elements are important or not. Unfortunately, as discussed above, the lack of convergence for the fitted force constants precludes any such test in this case, except for the nearest-neighbor interactions.

Because of the similarity in band structures, any successful theory of the lattice dynamics of copper could probably be applied to certain of the transition metals, such as nickel, as pointed out by Birgeneau *et al.*<sup>11</sup> However, for all these metals including copper, the influence of the high-lying  $d$  states on the lattice dynamics is uncertain. It is possible that the large  $3d$  cores might be polarized by the ionic displacements, as in the "shell-model" theory,<sup>44</sup> with additional complications arising from the interaction of the conduction electrons with the core polarizations.

*Note added in proof.* Recently Srivastava and Dayal [Phys. Rev. **140**, A1014 (1965)] have also calculated the dispersion relation in copper, using essentially Taya's theory and parameters, but with a different way of taking the exchange and correlation effects into account, and have obtained good agreement with the present neutron-scattering results.

#### ACKNOWLEDGMENTS

This work was carried out during the tenure of a Research Maintenance Grant from the Board of Research Studies, University of Cambridge, which is gratefully acknowledged. The author is grateful to Dr. P. A. Egelstaff for the use of the Cold Neutron Facility on the DIDO Reactor at Harwell, and for his kind cooperation, to Dr. G. Peckham and Dr. D. Long Price for invaluable help with the experiments, and to the members of the P.N.R. Group at Harwell for their assistance and cooperation. He also wishes to express his thanks to Professor W. Cochran, F.R.S. and Dr. J. R. Hardy for helpful discussions on the theory, and to Dr. G. L. Squires for the use of some of his computer programs, and for his continued help and encouragement.

<sup>42</sup> A. B. Pippard, Phil. Trans. Roy. Soc. London **A250**, 325 (1957).

<sup>43</sup> J. M. Ziman, Advan. Phys. **10**, 1 (1961).

<sup>44</sup> Cf., for instance, B. G. Dick, J. Phys. Chem. Solids, Suppl. **1**, 159 (1965).